Lab on a Chip

PAPER

View Article Online
View Journal | View Issue

Cite this: *Lab Chip*, 2026, **26**, 2035

WAFFLE – an automated platform for enhancing the performance of electrochemical biosensors

Alexandra Dobrea, *[ab] Rowan Blake,[c] Daniel Macdonald, [c] Cormack McKenzie,[a] Yoann Altmann,[d] Damion K. Corrigan [c] and Melanie Jimenez[b]

Electrochemical biosensors and microfluidics have an inherently synergistic relationship which can allow unparalleled levels of signal enhancement, automation and scalability. In spite of this, the full advantages of fluidic automation remain underexplored with most works automating some but not all biosensor fabrication steps. In this work, we present for the first time the Wee Ally for Flow Functionalisation of Low-cost Electrodes (WAFFLE) – an automated platform designed specifically for researchers to standardise the fabrication of electrochemical biosensors and enhance their performance, and a novel data analysis scheme based on the Markov chain Monte Carlo (MCMC) method for increasing the robustness of data fitting. We first discuss the design of the WAFFLE which features a modular construction, off-the-shelf components (ESP32 microcontroller, Bartels mp-6 μ-pump and memetis μ-valves), an easy-to-manufacture fluidic cartridge, and web interface that can be accessed from any Wi-Fi enabled device. The entire platform can be manufactured for approximately £1 k, less than the cost of a single standard syringe pump. We showcase the sensing benefits of the WAFFLE using two electrochemical immunoassays of high clinical relevance for interleukin-6 (IL-6) and cardiac troponin I (TnI), and one aptamer-based impedimetric assay for cortisol. As well as unilaterally enhancing the sensitivity of those sensors and decreasing sensor variability, the WAFFLE also highlighted some key insights into the assembly of the bioactive surface layer under flow. Finally, we demonstrate how MCMC-integration into impedance fitting algorithms can resolve the issue of local minima trapping.

Received 22nd October 2025,
Accepted 16th February 2026

DOI: 10.1039/d5lc00988j

rsc.li/loc

Introduction

Electrochemical biosensors are powerful tools that have had a profound impact on medical diagnostics and healthcare, particularly in diabetes management. With their commercial potential and scalability, there has been substantial interest in developing these sensors for a wide range of point-of-care applications, aiming to complement or replace more time consuming and expensive techniques such as ELISA or mass spectrometry.[1–5] However, their wider adoption beyond glucose monitoring is still untapped – with challenges remaining pertaining to sensor stability, assay multiplexing, reproducible formation of homogeneous and well-defined surface assembled monolayers (SAMs),[6–8] and detection sensitivity in complex media (*e.g.*, blood).[9]

Microfluidics has long been identified as an ideal candidate to solve some of these challenges, offering clear signal enhancement and automation benefits.[10–12] Systems based on digital microfluidics,[13–15] droplet microfluidics,[16,17] paper-based[18–20] or capillary-driven devices[21] for instance have all been proposed. Importantly however, most systems use microfluidics to enhance sample processing and/or automate some, but not all the biosensor preparation steps (Table S1), therefore not harnessing their potential for full assay automation, a factor critical towards in-field deployment. In our previous work, we confirmed that fluidic confinement can improve the electrochemical detection of a target molecule (~7-fold improvement in human serum),[22] but fluidic integration can also enhance the sensor preparation reliability.[23]

Electrochemical immunosensor preparation depends on the assay layout but typically comprises a series of steps for attachment of capture antibodies to the electrode surface *e.g.*, through spontaneous absorption or chemical modification, backfilling the surface to prevent non-specific interactions, sample addition, detection antibody attachment which may be conjugated with an enzyme *e.g.*, horseradish peroxidase or alkaline phosphatase and substrate addition

[a] *Biomedical Engineering Department, University of Strathclyde, Glasgow, G4 0NW, UK. E-mail: alexandra.dobrea@strath.ac.uk*
[b] *James Watt School of Engineering, University of Glasgow, Glasgow, G12 8QQ, UK*
[c] *Pure and Applied Chemistry Department, University of Strathclyde, Glasgow, G4 0NW, UK*
[d] *James Watt School of Engineering, Heriot-Watt University, EH14 4AS Edinburgh, UK*

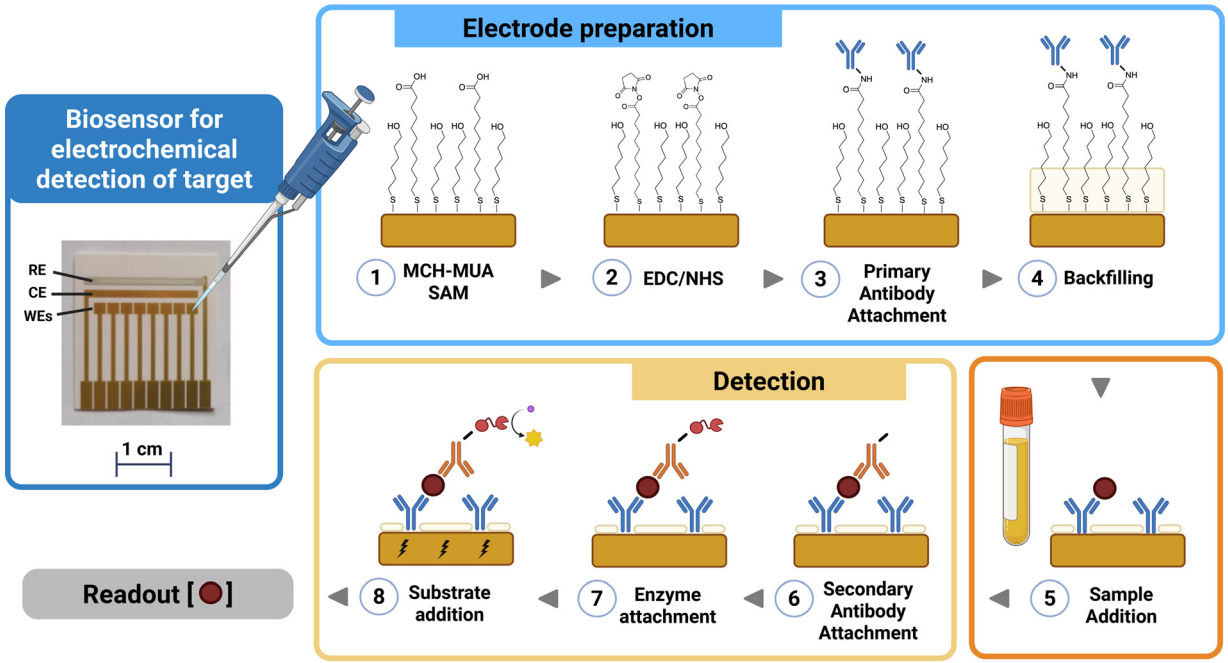

Fig. 1 Typical steps involved in preparing a sandwich-type electrochemical immunoassay using the standard *N*-(3-dimethylaminopropyl)-*N*′-ethylcarbodiimide/*N*-hydroxysuccinimide chemisorption mechanism. The electrochemical biosensor used in this work with the Ag/AgCl pseudoreference (RE), gold counter (CE) and 8 working electrodes (WE) is shown on the left. The preparation of these sensors involves the deposition of a thiol layer, in the case of this work a mixture of 11-mercaptoundecanoic acid (MUA) and 6-mercapto-1-hexanol (MCH), onto which the capture antibody is attached *via* carbodiimide chemistry. The surface is then backfilled to prevent non-specific binding before introducing the sample (*e.g.*, human serum) containing the target of interest which is captured by the antibodies present on the surface. A biotinylated secondary (or detection) antibody is then added which forms an immunocomplex with the captured target and primary antibody. An enzyme (*e.g.*, horseradish peroxidase) is then attached to the secondary antibody which in the presence of a chromogenic substrate (*e.g.*, 3,3′,5,5′-tetramethylbenzidine) gives rise to a coloured product which can be directly detected at the electrode surface. These steps are typically performed manually using pipettes or by submerging the electrodes in the required reagents. Created in BioRender. Dobrea, A. (2026) https://BioRender.com/pjsgvq5.

which is converted by the enzyme into a detectable signal (Fig. 1). These steps are commonly performed manually, generating an inherent sensor-to-sensor variability.[23] To explore automated sensor preparation (and thus minimise this variability) requires precise multiple-steps reagents control; this often relies in the literature on syringe pumps,[24–27] pressure controllers[28,29] and large multi-way valving systems,[29–31] all providing excellent accuracy but often sacrificing on device size and/or reagent volumes. Some papers have targeted this issue, providing solutions where multiple fluid routing is possible with a small device footprint and low reagent volumes. For instance, Zhao *et al.* demonstrated a plug-and-play fluidic system that can be interfaced directly with off-the-shelf electrodes (eSIREN), for the DNA-based detection of SARS-CoV-2 from swab lysates. Their system uses a small off-the-shelf pressure pump and a solenoid valve manifold controlled *via* a smartphone.[32] In a similar vein, Uludag and colleagues presented an integrated system for reagent dispensing over an electrode made in-house, demonstrating feasibility for *E. coli*[33] and prostate specific antigen[34] detection. However, for both platforms, only the final steps of the functionalisation procedure are performed using fluidics (steps 2–8 or 5–8 in Fig. 1). That is also the case for Dulay *et al.* which created an automated platform for electrochemical sensor preparation using multiple reagents reservoirs (each with their own in-line peristaltic pump)[35] and Kadimisetty *et al.* who produced an impressive platform based on a 3D printed fluidic chip with micropumps[36] (steps 5–8 in Fig. 1).

In this work, we propose a system that can perform the full electrochemical sensor preparation pipeline including the initial monolayer assembly automatically, along with readout. The system, named WAFFLE (**W**ee **A**lly for **F**low **F**unctionalisation of **L**ow-cost **E**lectrodes), has been designed to accommodate a variety of functionalisation procedures and electrode designs, relies on accessible fabrication methods and fully open-source documentation. The WAFFLE can be controlled by any Wi-Fi enabled device *via* its bespoke graphical user interface (GUI), and has been optimised for miniaturisation, low power consumption, and low dead volumes. The robustness of our approach not only relies on the hardware; we also developed a new signal processing pipeline relying on the Markov chain Monte Carlo (MCMC) algorithm to significantly improve the readout of the sensor. We demonstrate the advantages of the WAFFLE using 3 model assays: 2 electrochemical immunoassays for IL-6 and cardiac troponin respectively, and one impedimetric aptamer-based sensor for cortisol. For all assays, a significant decrease in coefficient of variation and increase in the detection sensitivity is reported thus confirming the potential

of the approach. The work provides a new avenue for biosensor fabrication standardisation that will ultimately facilitate technology translation.

We strongly believe that the WAFFLE, alongside this new approach to data fitting will become indispensable parts of the electrochemical biosensor researcher's toolkit.

Materials and methods

Chemicals and materials

Sulfuric acid (98%), *N*-hydroxysuccinimide (NHS), *N*-(3-dimethylaminopropyl)-*N*′-ethylcarbodiimide (EDC), sodium chloride (NaCl), magnesium chloride ($MgCl_2$), phosphate buffer (PBS) tablets, 6-mercapto-1-hexanol (MCH), 11-mercaptoundecanoic acid (MUA), fluorescein, potassium ferricyanide (99%), potassium ferrocyanide trihydrate (99%), tris(2-carboxyethyl)phosphine hydrochloride, hydrocortisone, 0.2 μm Whatman filters and HPLC-purified aptamer sequences[37] (Table S2) were purchased from Merck. Gibco™ PBS, 0.5 M MES buffer (pH 5.5) and molecular grade water were purchased from Fisher Scientific. The ultrapure water (18.2 MΩ cm) used in the experiments was from an Elga Purelab Chorus water purification system. IL-6 primary and secondary antibodies, target protein and streptavidin-linked horseradish peroxidase were part of the Human IL-6 DuoSet ELISA kit (DY206) and were purchased together with the reagent diluent (1% w/v BSA in PBS), pre-made TMB substrate with hydrogen peroxide (DY999B) and plate coating buffer (DY006) from Biotechne R&D Systems. Troponin primary (19C7) and HRP-labelled secondary antibodies (4C2) were purchased from Novusbio and Biotechne respectively. Recombinant human troponin I standards (8ICR2) and troponin-depleted human serum (8TFS2) were purchased from Hytest.

Fluidics. Mini luer fluidic connectors (male and female), silicone tubing, 0.2 and 4.5 ml reservoirs, luer to mini luer fluidic adaptors were purchased from microfluidic ChipShop (Jena, Germany). Mp-6 micropumps, mp-damper, Takasago valves and the mp-lowdriver chip were purchased from Bartels Mikrotechnik (Dortmund, Germany), the normally closed memory shape alloy valves were from memetis GmbH (Karlsruhe, Germany) and the flow sensor from Sensirion AG (Switzerland). The mp-valveDriverM and mp-valveDriverT were purchased from Darwin microfluidics. 3 mm thick PMMA sheets were purchased from Stockline Plastics Ltd (Glasgow, UK), 0.1 mm thick PET spacer layers from ZHluja (Amazon UPC 766972224591) and adhesive transfer tape was purchased from 3M™ (468MP). PMMA sheets are laser cut to the correct dimensions using an Epilog Mini 50 W laser cutter while PET sheets are cut using a Cricut Maker 3.

WAFFLE system design and validation

The full protocol to build the WAFFLE step-by-step and all the design files have been uploaded to the following repositories: https://github.com/ADobrea797/WAFFLE (GitHub) and https://doi.org/10.5281/zenodo.17877849 (Zenodo).

Instrumentation. Multiplexing for the valves is achieved using a TPIC6C595 shift register (Texas Instruments) with an SQ2364EES-T1 MOSFET (Vishay Intertech) on each valve control line acting as an electronic switch. The 3 drivers and flow sensor are controlled by an ESP32-S2-Mini development board (Espressif Systems) *via* the I2C communication protocol, while the shift register is controlled *via* the SPI interface. The graphical user interface takes the form of a website and is created using HTML. The Arduino PID control library by br3ttb (https://github.com/br3ttb) was used in the code to automatically adjust the voltage amplitude of the pump to return the desired flow rate. To minimise the number of wires and size of the controller, the electrical circuit was converted into a PCBA format using the KiCad software and ordered from JLCPBC (Hong Kong, China). All the components were installed in a plastic enclosure designed in Autodesk Fusion360 and 3D printed using a Creality Ender 3 V3 KE printer in white hyper PLA filament.

Flow characterisation. To characterise the flow rate generated by the mp-6 micropump, flow sensor data was displayed in real time in the ArduinoIDE serial monitor and automatically captured in an Excel worksheet using the Parallax Data Acquisition (PLX-DAQ) tool. The flow rate was characterised across all the inlets in triplicate. To assess washing efficiency, the system was filled with either concentrated fluorescent dye or 2 mM ferri-ferrocyanide solution and then flushed with clean filtered 1× PBS. The decrease in fluorescent signal intensity over time at varying flow rates was monitored *via* video recording using a Dinolite tabletop digital microscope, with images analysed using ImageJ. For the ferri-ferrocyanide solution washout, the decrease in the peak current of the differential pulse voltammogram data over time at varying flow rates was recorded using a PalmSens4 potentiostat and laptop running the PSTrace 5.10 software.

Electrochemical sensor preparation

Electrode platform. The gold (Au) sensors used in this work are from FlexMedical Solutions (Livingston, UK) and they each contain 8 working electrodes and 1 common Au counter and silver/silver chloride (Ag/AgCl) reference electrode per chip (Fig. 1). Before use, all sensors were rinsed with deionised (DI) ultrapure water and dried under stream of argon, before being cleaned by 10 cycles of voltage cycling (0–1.6 V) in 0.1 M sulfuric acid using a voltage step of 0.02 V and scan rate of 0.2 V s^{-1}. Following this, the sensors are rinsed again with DI water and dried under argon before being placed in a clean storage box until ready to be used, which is always on the same day.

IL-6 and troponin detection. A 1 : 4 mixture of MUA and MCH (200 μM MUA : 800 μM MCH) is prepared in 20% (v/v) ethanol and 80% (v/v) 1× PBS and incubated for 1 h at room temperature with TCEP in a 1 : 5 thiol to TCEP ratio to reduce

the terminal disulphide bond and allow effective gold attachment. This solution is then pipetted to cover all 8 working electrodes (for manual preparation) or introduced using flow (for WAFFLE preparation) to the sensing area and incubated overnight at 4 °C in a humidity chamber (critical for the manually prepared sensors to prevent evaporation but not needed for the sensors prepared with fluidics). The next day, unreacted thiols are washed away using 3 ml of DI water dispensed using a pipette for the manually prepared electrodes or by flowing in DI water using the WAFFLE set to dispense 3 ml min^{-1} for 1 minute. A solution containing 5 mM EDC and 15 mM NHS in 0.1 M MES buffer is then introduced to the sensing area (using a pipette or flowing in for 15 s at 2 ml min^{-1}) and incubated for 15 minutes at room temperature. Next, the EDC/NHS solution is taken off without washing and 12.5 μg ml^{-1} primary antibodies are placed on the sensing area. Alternatively, for the WAFFLE, the antibodies are flown in directly after the EDC/NHS solution at 2 ml min^{-1} for 15 s. Sensors are then incubated for 1 h at room temperature. Following this incubation step, as well as in-between all the remaining steps, the sensors are washed with 1× PBS (Gibco™) using 3 ml pipette-dispensed for manual preparation or using a 2 ml min^{-1} flow rate for 1 minute. The sensors are then backfilled using reagent diluent (1% w/v BSA in PBS, pH 7.2–7.4, 0.2 μm filtered) for 1 hour at room temperature. The samples (PBS or neat serum) containing the target protein (troponin or IL-6) are then introduced, followed by secondary antibody addition and incubation for 1 hour each at room temperature. For the IL-6 assay, this is followed by a 20 minute incubation with 1× streptavidin-HRP in the dark at room temperature. Finally, the sensor is washed for one final time before introducing the substrate solution – a pre-made mix of tetramethylbenzidine (TMB) and H_2O_2 and incubated for 20 minutes in the dark before measuring the solution by performing chronoamperometry at −0.2 V, 0.1 s time interval for 60 seconds. The value of the stabilised current for each measurement at 60 seconds is then extracted for data analysis and plotting. The limit of detection (LoD) was defined as the first experimental datapoint falling outside the ±3 standard deviation zone around the average blank reading (0 pg ml^{-1} target).

Cortisol detection. For the cortisol electrochemical aptamer-based (E-AB) sensor, 2 μl of 100 μM anchor aptamer was incubated with 10 mM TCEP in a 1 : 1 volumetric ratio for 1 h at room temperature. The anchor aptamers were then diluted to the working concentration (200 nM) using aptamer buffer (1 M NaCl, 10 mM $MgCl_2$, 5 mM KCl in molecular grade water, pH 7.5)[37] with 0.1% (v/v) Tween-20 surfactant. 2 μl of aptamers were then pipetted on each working electrode and the sensors were placed inside a humidity chamber and incubated overnight at 4 °C. For the WAFFLE, the aptamers were delivered to the sensing area using flow. The following day, excess unbound aptamers were washed off using 3 ml of aptamer buffer dispensed using a pipette for the manually prepared sensors or by flowing in buffer at 2 ml min^{-1} for 3 minutes. Next, the surface was backfilled using 1 mM MCH pipetted over the working electrodes or flown in at 2 ml min^{-1} for 15 seconds before another overnight incubation at 4 °C. The third day the electrodes were again washed to remove unbound thiols. Cortisol specific aptamers were then diluted to 1 μM using aptamer buffer (1 : 5 ratio of anchor to detection aptamer) and folded by heating up to 95 °C for 5 minutes using a miniPCR machine (miniPCR bio). Following this, the aptamers were allowed to reach room temperature before being introduced to the sensing surface and incubated for 2 h at room temperature. Finally, after a final washing step, cortisol spiked aptamer buffer was introduced to the sensing area and incubated for a further hour. An impedance spectroscopy measurement was taken after the last 2 steps, before and after the addition of cortisol, against the open circuit potential, using 61 frequencies between 0.1 Hz and 100 kHz. All electrochemical data in this study is acquired using a PalmSens4 potentiostat with a MUX8-R2 multiplexer unit from PalmSens (Houten, Netherlands).

Data analysis and plotting

Impedance data was fitted using Randles equivalent circuit model incorporating a constant phase element rather than an ideal capacitor to account for non-ideal sensor behaviour. Data fitting was performed either using the standard fitting tool of PSTrace 5.10 or the open-source impedance fitting code Zfit by Jean-Luc Dellis modified with the Markov chain Monte Carlo (MCMC) algorithm (full code was uploaded on GitHub and Zenodo). All data was then exported, plotted and analysed using GraphPad Prism 10. Where only 2 distributions are compared, for instance in the manual *vs.* WAFFLE graphs, a student's *t*-test was used to determine statistical significance. Where multiple comparisons were made, *e.g.*, a control group against multiple sequential treatments, a one-way ANOVA with a Tukey *post hoc* test was used.

Results and discussion

This work proposes to integrate all the commonly manual steps depicted in Fig. 1 for electrochemical sensing in the automated, portable WAFFLE platform. The platform comprises 1) a flow cell to allow fluids to pass on top of the electrodes as described in our previous work,[22] 2) a carousel to handle all the reagents and buffers required to perform the electrode preparation and assay of choice, 3) an electronic control board, and 4) a user interface. Full instructions for manufacturing the WAFFLE have been uploaded to GitHub and are available at https://github.com/ADobrea797/WAFFLE, with examples of processing in Video S1.

WAFFLE features

The WAFFLE features reservoirs for all the reagents required for preparing a typical sandwich immunoassay: for instance, thiol molecules for SAM formation, EDC/NHS linker, primary and secondary antibodies, backfilling agent, enzyme label,

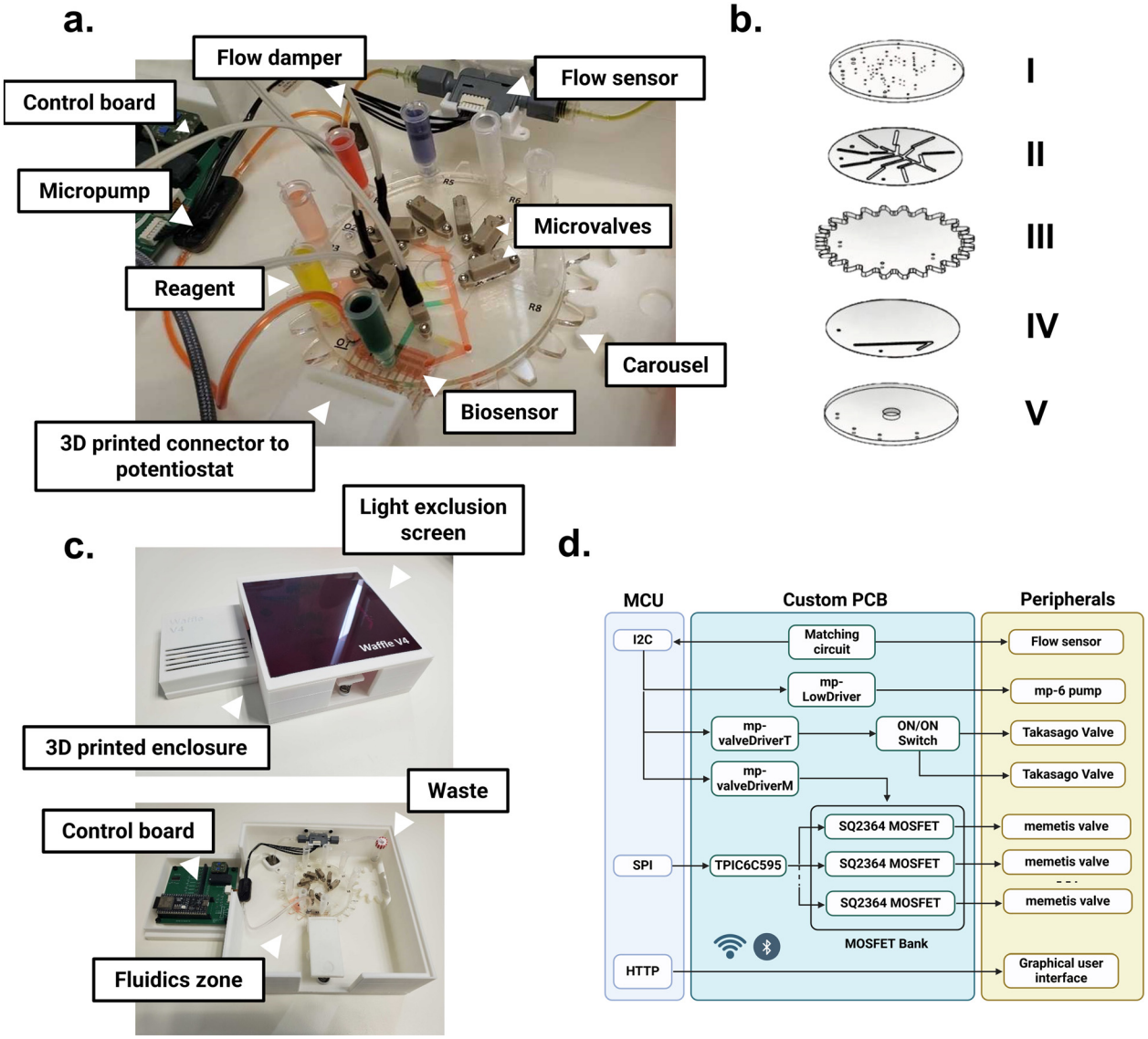

Fig. 2 The Wee Ally for Flow Functionalisation of Low-Cost Electrodes (WAFFLE) platform. (a) Reagents cassette employing the memetis normally closed memory shape alloy valves, flow cell interfacing the electrochemical sensor, reagent reservoirs, tubing and fluidic adaptors. The flow is actuated using an mp-6 micropump, Sensirion flow sensor and electronic control board (b) Exploded assembly of the multilayer reagents cassette which includes (I) inlets layer with holes for the reservoirs and in-line valves – 3 mm thick laser cut PMMA, (II) channels layer connected to the memetis valves for reagent selection – 2 layers of double-sided adhesive with a PET spacer, (III) middle layer with spur gear profile for allowing rotation to the next electrode under test and inlet holes for access to the fluidic channel on the bottom side – 3 mm thick laser cut PMMA, (IV) flow cell splitter channels for selection of the desired flow cell to receive the reagent/buffer – double sided adhesive with PET spacer, (V) flow cell inlet/outlet layer to which the electrode is attached *via* double sided tape delineating a channel on top of the electrodes. (c) 3D printed WAFFLE enclosure with semi-opaque lid for protecting light sensitive reagents. A two-chamber design with the electronics placed at a slightly higher elevation was employed to separate the electronics from the fluidics (top). The inside of the WAFFLE showing placement of components such as electrode connector, flow damper, flow sensor *etc.* (bottom) (d) High level diagram of the electronic control unit using a bank of SQ2364 MOSFETs with a TPIC6C595 open drain shift register for valve selection *via* the user interface and the drivers used for controlling the actuators (Created in BioRender. Dobrea, A. (2026) https://BioRender.com/pjsgvq5).

sample and chromogenic substrate (n = 8 reagents in total). Each reservoir connects to a side channel that feeds into a larger main channel that directs the flow over the surface of the biosensor (Fig. 2a). An exploded view of the fluidic cartridge and the final assembled device can also be seen in Fig. 2b and c. Each side channel features a memetis valve, which allows the selection of the required reagent. A mp-6 micropump is located downstream of the sensor actuating the flow with the help of a Sensirion flow sensor and flow damper. The damper serves to smooth the pulsatile flow created by the pump allowing the flow sensor to record an accurate reading. The placement of the pump downstream of the electrodes is to minimise the dead volume introduced into the system. The signal required for driving the mp-6 pump is generated using the mp-lowdriver integrated circuit (IC) chip which can provide the required waveform for

running the pump up to 150 V amplitude and 2000 Hz frequency. This IC was chosen due to its easy integration and low power requirements which make it suitable for battery powered devices. Although the applied frequency can also be adjusted to modulate the flow rate (Fig. S1), this was locked in this study at 100 Hz as per the manufacturer's recommendation for water-based liquids and flow rate setting was driven by the voltage amplitude applied to the micropump. The voltage amplitude generated by the mp-lowdriver is adjusted in real time using a proportional-integral-derivative (PID) element. To minimise the risk to users as the electronics operate at high voltages, the electronics and fluidics were housed inside of a 3D printed plastic enclosure with the fluidic zone designed to be slightly lower than the electronics zone to prevent risks associated with leaks (Fig. 2c). A dark tinted semi-transparent lid was also laser cut and installed into the 3D printed frame to protect light sensitive reagents (*e.g.*, TMB) while allowing the user to see the fluidic operations. As the ESP32 MCU controlling the system (Fig. 2d) is Wi-Fi enabled, the graphical user interface (GUI) created is a website which can be simply accessed by inputting the unique IP address of the microcontroller *e.g.*, 'http:/192.XXX.XX/' into the preferred web browser. By controlling all the functions using a webpage interface, the need for additional peripherals (*e.g.* LCD screen, push buttons, LEDs) is removed which improves long term device reliability, and user accessibility is promoted through the use of free, open access software (*e.g.*, ArduinoIDE) for running the device (Video S1).

The total cost for one WAFFLE, without valves is ~£400 (544 USD). This price can be further decreased to ~£150 (204 USD) by designing the drivers (AC voltage and constant current generators) from scratch rather than buying them off the shelf. Currently, the valves are the priciest element at £88.40 (120 USD) per unit. While enabling smooth automation, the valving system can be simplified, *e.g.*, by using manual valves.

Fluidic characterisation

Preliminary data demonstrated some flow fluctuations across different reagent inlets (Fig. S2), prompting the addition of a PID controller. After calibration (Fig. S3), k_p = 5, k_i = 15, k_d = 1 were the chosen parameters to produce a rapid response (<20 s) with a steady state error of ~0.5% for all the inlets (Fig. 3a and b). The system was found stable in the 0.1–2.5 ml min^{-1} range (Fig. 3c), the upper limit being imposed by the flow sensor.

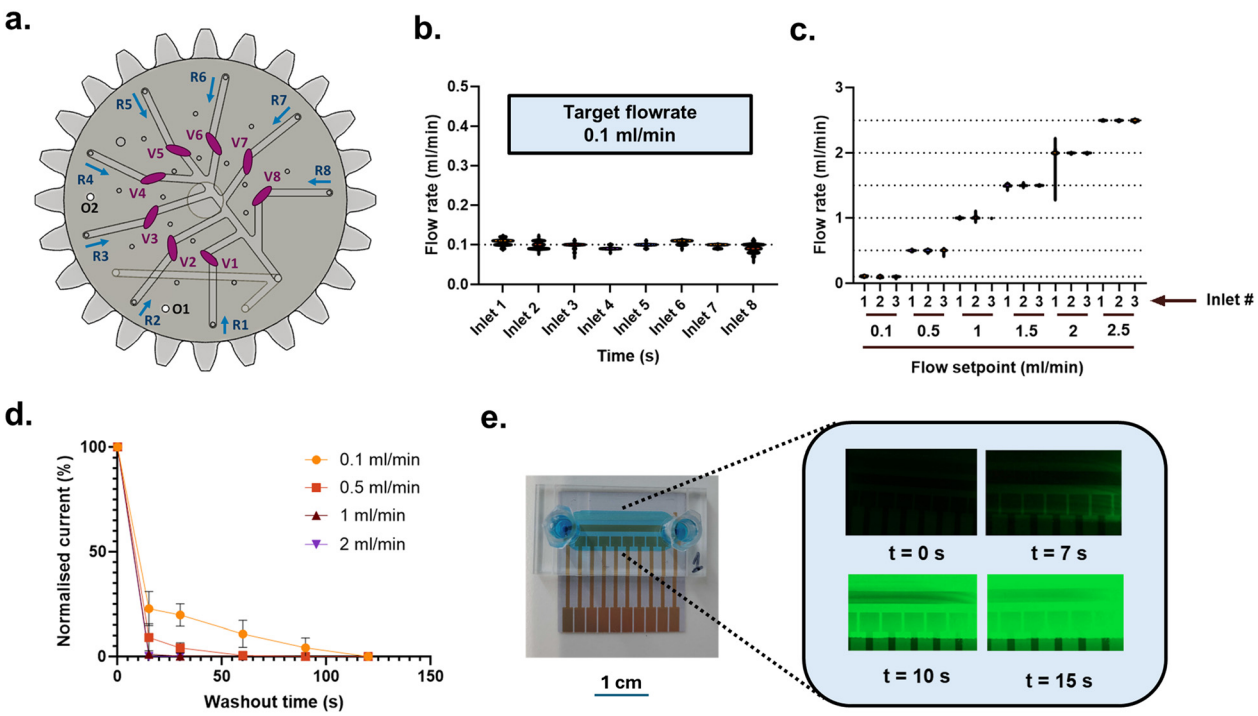

Fig. 3 WAFFLE fluidic characterisation. (a) Schematic view of the reagent cartridge with individual reagent lines (R1–8), microvalves (V1–8) and outlets (O1 and 2) (b) Returned flow rates across the different inlets of the reagent cassette for a set point flow rate of 0.1 ml min^{-1}. Proportional-integral-derivative (PID) control integrated into the platform code allows automatic selection and real time adjustment of the voltage amplitude provided to the pump allowing automatic harmonisation of the flow rate across the different branches of the fluidic cassette. (c) PID control allows the selection of a wide range of setpoint flow rates with a <20 s response time. (d) Washout times required by different flow rates to replace 1 mM ferri-ferrocyanide in 1× PBS with clean buffer over the biosensor surface – a proxy experiment for sequential delivery of different reagents to the biosensor surface. The signal was monitored using the peak current of the differential pulse voltammogram. (e) Fluorescence microscopy images acquired showing the middle of the flow channel on top of the electrodes while fluorescent dye is flown in at 1 ml min^{-1} flow rate (inlet is on the right side).

Since the preparation of electrodes revolves around sequential addition of reagents with washing phases in between, the system then had to be calibrated for washing time (*i.e.*, time needed to fully fill or empty the sensor with a specific reagent). Washing times were consequently characterised using a standard redox media consisting of 2 mM ferri-ferrocyanide or a fluorescent dye flushed by PBS. Fig. 3d shows that it takes ~15 seconds at 1 and 2 ml min^{-1} to remove the redox couple and return to the baseline current of clear PBS. These results were in agreement with data acquired using the dye, with the channel fully fluorescent after ~15 s (Fig. 3e, Video S2). All the assays presented hereafter are consequently done with a flow rate of 2 ml min^{-1} for 15 seconds for reagents loading/unloading.

Sensing advantages of the WAFFLE

The full automation of the WAFFLE was first tested for the detection of inflammation marker IL-6. To evaluate the antibody loading density on the electrode surface, impedance data of the functionalised surface was probed with a standard ferri-ferrocyanide couple, and the response was fitted with Randles equivalent circuit. The R_{ct} value increased from 246.8 ± 148.5 kΩ to 579.1 ± 71.7 kΩ and the coefficient of variability was reduced from 0.60 to 0.12 when the sensors were prepared with the WAFFLE platform compared to manual preparation (Fig. 4a). This suggested a higher antibody loading density and more uniform and reproducible SAM formation across the different electrodes. Furthermore, compared to the standard preparation of electrodes (fully manual and without any microfluidic component), the WAFFLE displays a significant boost in signal for the IL-6 dose response in PBS (Fig. 4b). The LoD decreased from ~400 to 211 pg ml^{-1} with the WAFFLE preparation, and a sensitivity increase of 2.6-fold was observed over the linear range of the sensor. A similar signal enhancement was found in human serum, with a 4-fold increase in sensitivity when the sensor is prepared fully automatically (Fig. 4c). This signal enhancement might be linked to the creation of an antibody layer on the surface of the electrodes that is less variable (perhaps due to the minimisation of environmental contamination and evaporation) compared to manual preparation, and with a higher antibody loading. The signal enhancement could be translated to other assays. For troponin for instance, a cardiac biomarker, a signal enhancement of ×1.67 was recorded in serum (Fig. S4). This enhancement could probably be further increased by further optimising the flow regime or antibody attachment chemistry to the gold surface (Fig. S4c).

For cortisol sensing, the mechanism of attachment to the electrode and detection principle is different. As opposed to the previous assays, the sequence of automation of the WAFFLE needs to include 1) anchor aptamer attachment, 2) backfilling the surface to prevent non-specific binding, 3) immobilisation of the cortisol specific aptamer, 4) sample introduction and 5) readout of the impedance signal through the introduction of a redox mediator (Fig. 5a). The aptamer loading density to the electrode surface was lower when preparing the sensors with the WAFFLE compared to manually; however, the variability of these sensors was drastically reduced for both the anchor attachment (Fig. 5b) and the duplex formation (Fig. 5c). Interestingly, the response recorded with WAFFLE-prepared sensors did not match the expected behaviour from a strand displacement impedimetric system, where the charge transfer resistance would be expected to decrease in the presence of the target. It appears that in our system the presence of cortisol has an anchoring effect; this might be due to the increased dwelling time in the buffer containing $MgCl_2$, preventing the removal of the cortisol aptamers by flow. While more work would be needed to understand this phenomenon, the data still demonstrate an increased sensitivity for cortisol detection in our system (Fig. 5d).

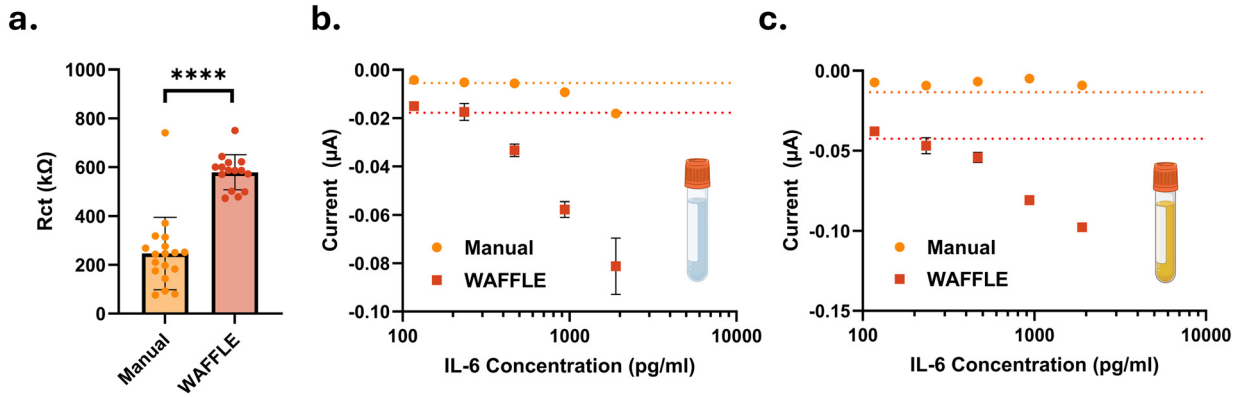

Fig. 4 Comparison between manual and WAFFLE-made electrochemical sensors with antibodies attached *via* EDC/NHS coupling. (a) The difference between an IL-6 antibody layer deposited on the electrode surface manually *via* pipetting or using the WAFFLE showing that performing all the functionalisation steps automatically increases the amount of antibodies attached to the surface (n = 16). R_{ct} values were determined by fitting the impedance response with Randles equivalent circuit. (b) Dose responses of WAFFLE and manually made sensors to increasing concentrations of IL-6 spiked in PBS and (c) neat human serum. Each marker represents the average over 8 electrodes ± 1 SD. Dashed lines represent the average blank reading – 3SDs (n = 8) and are used to determine the experimental limit of detection. **** – $p \leq 0.0001$. Blank averages with standard deviations for b and c can be found in Table S3. Insets in b and c were created in BioRender by Dobrea, A. (2026) https://BioRender.com/pjsgvq5.

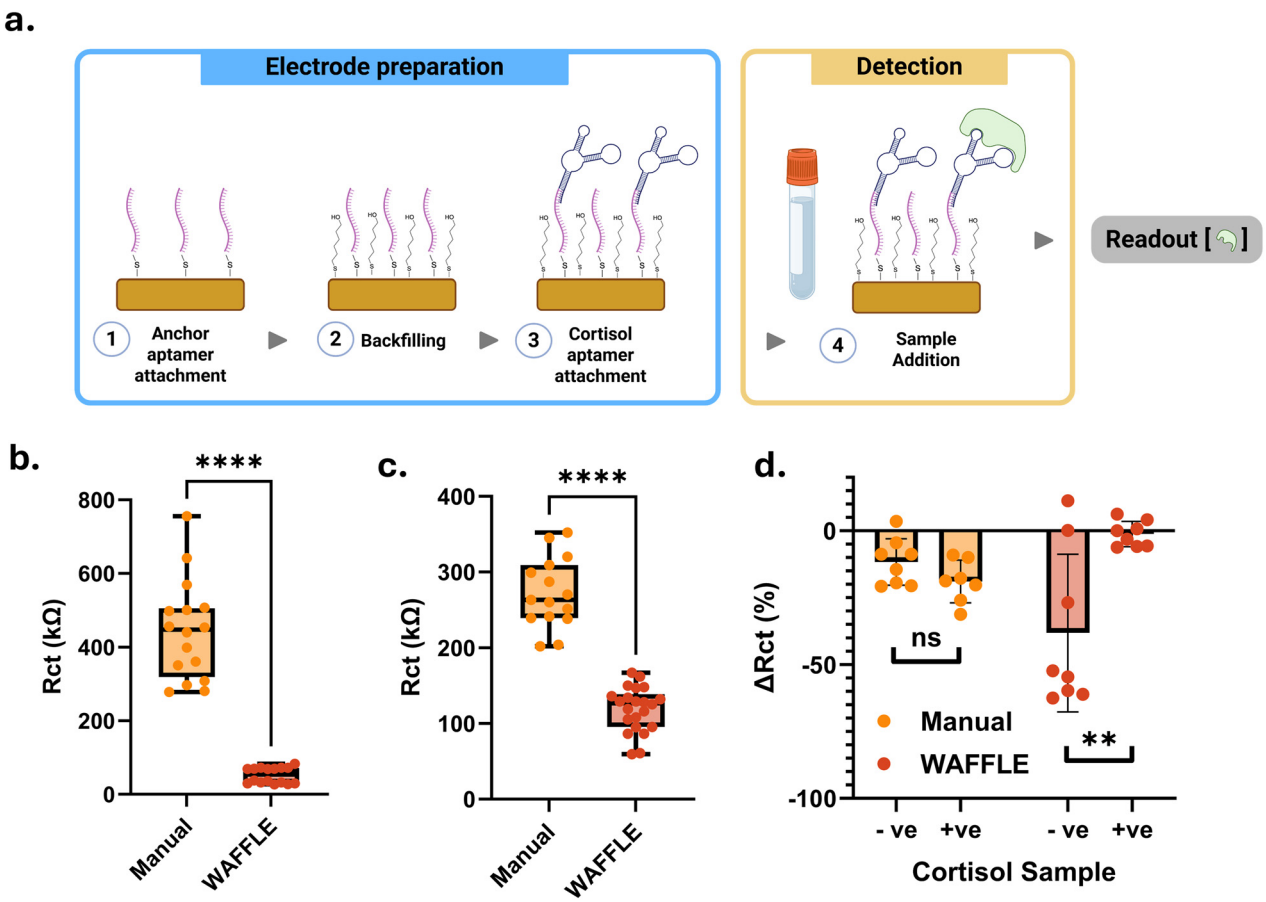

Fig. 5 (a) Schematic representation of the steps involved in preparing the cortisol aptasensor. The process involved attaching the anchor aptamer to the gold electrode surface *via* a thiol termination at the 5′ end. The surface is then backfilled using 6-mercapto-1-hexanol (MCH) before attaching the cortisol specific aptamer. Upon addition of the sample containing the target, the interaction between cortisol and its specific aptamer gives rise to a measurable change in the impedance characteristics of the bioactive surface (Created in BioRender. Dobrea, A. (2026) https://BioRender.com/pjsgvq5). (b) Comparison between aptamer deposition (direct aptamer attachment *via* thiol termination) using the WAFFLE *versus* manual preparation. (c) Comparison between aptamer deposition (full duplex assembly with mercaptohexanol backfill) using the WAFFLE *versus* manual preparation. (d) Cortisol spiked in aptamer buffer detection using aptasensors prepared manually *versus* with the WAFFLE platform. Data was fitted using Randles equivalent circuit in PsTrace 5.10. −ve represents a blank sample *i.e.* 0 pg ml^{-1} cortisol and +ve is a high cortisol concentration *i.e.* 23 ng ml^{-1}. ns – $p > 0.05$, * – $p \leq 0.05$, ** – $p \leq 0.01$, *** – $p \leq 0.001$, **** – $p \leq 0.0001$. Box plots display the interquartile range (IQR), the straight line denotes the median and the whiskers represent the minimum and maximum values recorded.

The WAFFLE can, in its current format, help save one hour per sensor with the ability to run two sensors simultaneously. The system has been designed to enable expansion, with up to 6 sensors fitting the system (or more with sensors with a smaller footprint).

Markov chain Monte Carlo impedance data fitting

We have demonstrated so far that the WAFFLE is a hardware solution capable of improving the sensitivity and reliability of electrochemical sensors for a range of detection assays. As previously mentioned, beyond the hardware, data fitting is a key component to extrapolate an analyte concentration. This is typically performed using black box proprietary software also used for running the potentiostat (*e.g.*, PsTrace) or equivalents,[38–44] but these tend to be strongly sensitive to initialisation values, frequently leading to sub-optimal fits due to local minima. To promote robustness throughout the whole sensing process, we propose a new fitting approach using MCMC. MCMC has been widely employed for quantifying uncertainties of data fitting, by cycling through the parameter space within defined upper and lower bounds. By using this statistical approach, the most likely fitting parameters can be extrapolated and we show that the method is robust to various initialisation conditions. To the best of our knowledge, we propose the first open-source code to tap into the unique capabilities of MCMC to solve data fitting challenges for impedance spectroscopy. While these capabilities are demonstrated here with the WAFFLE, the code can be used on its own for any assay relying on model fitting. Fig. 6 compares side by side impedance data fitted using PSTrace 5.10 (PalmSens proprietary software) and the proposed MCMC approach for the 3 assays tested here (IL-6, first row; troponin, second row; cortisol, third row). The

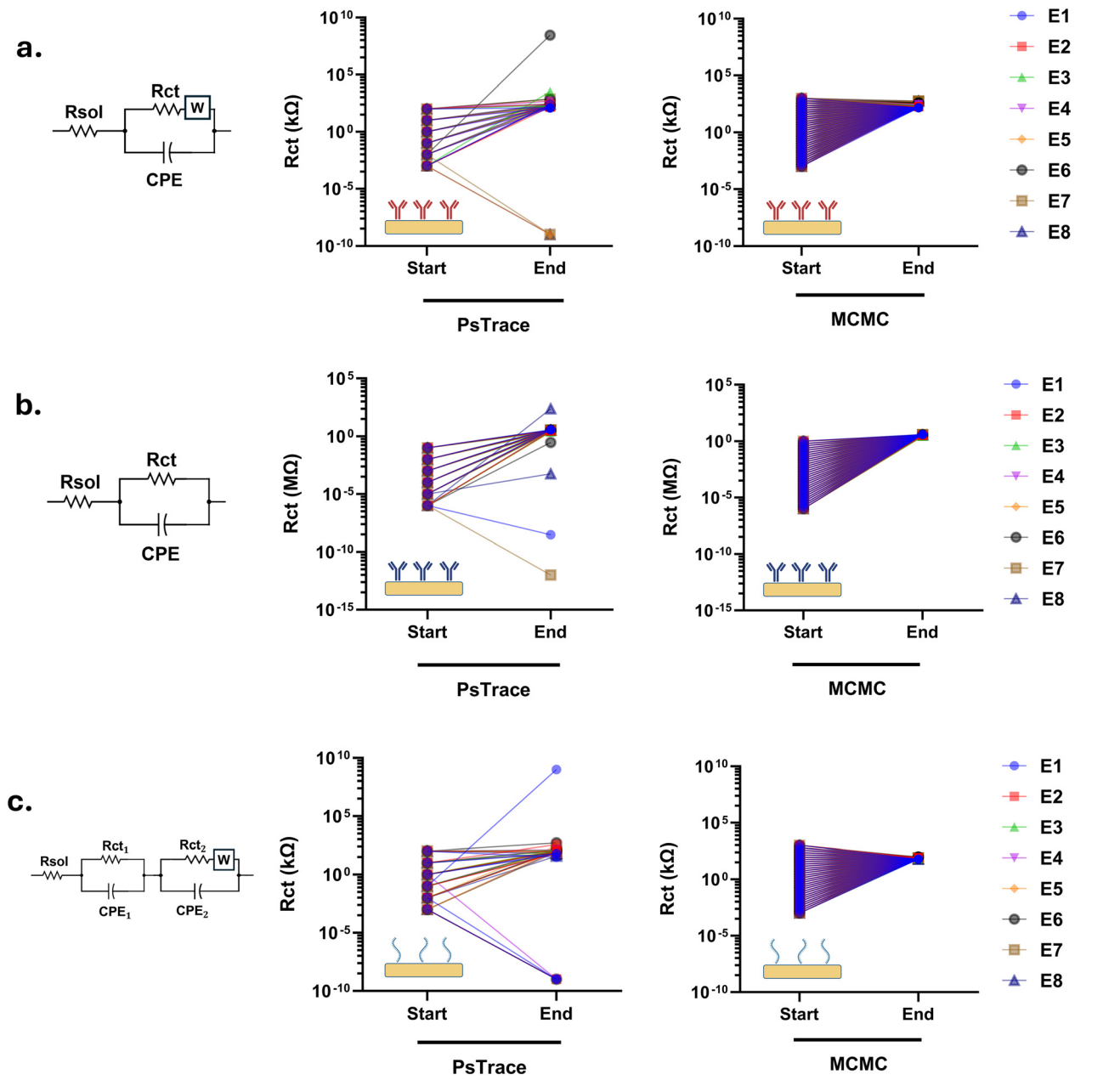

Fig. 6 Comparison between different impedance responses fitted using a standard 'black box' proprietary software (PSTrace 5.10; middle column) and a modified version of Zfit using the Markov chain Monte Carlo (MCMC) algorithm (right column). (a) Standard Randles equivalent circuit featuring the solution resistance (R_{sol}) in series with a parallel arrangement of the charge transfer resistance (R_{ct}), Warburg element (W) and a constant phase element (CPE). R_{ct} values represent 8 different working electrodes functionalised with IL-6 primary antibodies immobilized by physisorbtion. (b) Randles equivalent circuit without the Warburg element. R_{ct} values represent 8 different working electrodes functionalised with troponin I primary antibodies immobilized by EDC/NHS coupling. (c) Double RC grouping modelling a double semicircle impedance response. R_{ct} values refer to 8 different working electrodes functionalised with thiolated capture aptamers. Data fitted in PSTrace 5.10 uses different initialisation ('Start') values for R_{ct} (1–100 000 Ω) while all other parameters were initialised as unit value and shows the values on which the algorithm converges ('End'). Data fitted in the MCMC-modified Zfit algorithm uses a larger (10^4) input sampling pool between predefined parameter bounds which was illustrated by the larger line density in the right column. Insets were created in BioRender. Dobrea, A. (2026) https://BioRender.com/pjsgvq5.

electrical model for each assay was estimated using the observed impedance behaviour (raw Nyquist plots of the impedance spectra in Fig. S5): Randles equivalent circuit with and without a Warburg element and a double parallel RC grouping in series with a resistor. These datasets were specifically selected for this exercise as they are more challenging to fit and/or assess visually (*e.g.*, by not having a clearly defined inflexion point at the end of the semicircle, or between a double semicircle response). The initialisation value of R_{ct} was varied from 1 to 100 000 Ω to compare performances, while all other parameters were locked in at unit value. As demonstrated in Fig. 6a–c, optimisation using

PSTrace can lead to significant variation in R_{ct} estimation (average CoV ~0.92) depending on the initialisation. By contrast, the MCMC approach exhibits significantly less sensitivity, providing a consistent estimation for all the tested initialisation values, and for all the models tested. This approach consequently adds an extra layer of robustness, complementing the WAFFLE for a complete electrochemical process. The full code with 3 example circuits is available at https://github.com/ADobrea797/WAFFLE and can be adapted for wider use within the community.

Conclusions

Electrochemical biosensors have already transformed medical diagnostics and are likely to continue to do so in the coming decades. While significant research efforts are directed towards the development of these sensors and their underlying chemistries, microfluidic integration remains an underrepresented topic in the electrochemical biosensing community and its potential for full assay automation has not been fully explored. We hope to help address this by providing two new tools: the WAFFLE, an automated fluidic platform that replaces the manual steps associated with fabricating these sensors (pipette dispensing of reagents and washing) and a novel framework for analysing impedance data – one of the fundamental steps employed in electrochemical biosensor development. With the WAFFLE, we demonstrate a notable decrease in the variability of the bioactive surface monolayer and enhancement of the signal generated compared to manual preparation. We also uncovered some interesting insights into the assembly of the active surface detection layer under flow – a topic of much interest in the electrochemical biosensing community. We also demonstrated that the robustness of impedance fitting can be substantially improved by using MCMC. Together, we strongly believe that these two innovations could represent a fundamental shift in the way electrochemical biosensors are developed and provide a springboard for accelerating their development and deployment to the point of need.

Author contributions

(AD) conceptualisation, data curation, formal analysis, investigation, methodology, project administration, software, validation, visualisation, writing – original draft and review & editing; (RB) methodology, writing – review & editing; (DM) investigation, methodology, validation, writing – review & editing. (CM) investigation, methodology, validation; (YA) software (DC) conceptualisation, funding acquisition, project administration, supervision, writing – review & editing; (MJ) conceptualisation, formal analysis, funding acquisition, project administration, resources, software, supervision, writing – original draft and review & editing.

Conflicts of interest

There are no conflicts to declare.

Data availability

The data supporting this article have been included as part of the supplementary information. The code for operating the WAFFLE, impedance data loading and MCMC analysis can be found at https://github.com/ADobrea797/WAFFLE/tree/main. The version of the code employed for this study is version 0.

Supplementary information (SI) is available. See DOI: https://doi.org/10.1039/d5lc00988j.

Acknowledgements

A. D. would like to thank EPSRC for her support (EPT517896.1). This project was supported by the Royal Academy of Engineering under the Research Fellowship programme (RF201718.1741). A. D., D. C. and M. J. would also like to thank Tenovus Scotland for providing funding for this project (S19-23). A. D. would like to thank FabLab@Strathclyde for their help with manufacturing the flow cells.

References

1 F. Cui, Z. Zhou and H. S. Zhou, Review—Measurement and Analysis of Cancer Biomarkers Based on Electrochemical Biosensors, *J. Electrochem. Soc.*, 2020, **167**, 037525.
2 M. A. Khaleque, *et al.* Bioreceptor modified electrochemical biosensors for the detection of life threating pathogenic bacteria: a review, *RSC Adv.*, 2024, **14**, 28487–28515.
3 A. Sajeevan, R. A. Sukumaran, L. R. Panicker and Y. G. Kotagiri, Trends in ready-to-use portable electrochemical sensing devices for healthcare diagnosis, *Microchim. Acta*, 2025, **192**, 80.
4 Z. Saldaña-Ahuactzi, *et al.* Advancing foodborne pathogen detection: a review of traditional and innovative optical and electrochemical biosensing approaches, *Microchim. Acta*, 2025, **192**, 102.
5 H. Sable, *et al.* Review—Nanosystems-Enhanced Electrochemical Biosensors for Precision in One Health Management, *J. Electrochem. Soc.*, 2024, **171**, 037527.
6 D. K. Corrigan, *et al.* A microelectrode array with reproducible performance shows loss of consistency following functionalization with a self-assembled 6-mercapto-1-hexanol layer, *Sensors*, 2018, **18**(6), 1891.
7 A. Butterworth, *et al.* SAM composition and electrode roughness affect performance of a DNA biosensor for antibiotic resistance, *Biosensors*, 2019, **9**(1), 22.
8 D. Bizzotto, I. J. Burgess, T. Doneux, T. Sagara and H. Z. Yu, Beyond Simple Cartoons: Challenges in Characterizing Electrochemical Biosensor Interfaces, *ACS Sens.*, 2018, **3**, 5–12.
9 J. Wu, H. Liu, W. Chen, B. Ma and H. Ju, Device integration of electrochemical biosensors, *Nat. Rev. Bioeng.*, 2023, **1**, 346–360.
10 A. Fernández-la-Villa, D. F. Pozo-Ayuso and M. Castaño-Álvarez, Microfluidics and electrochemistry: an emerging

tandem for next-generation analytical microsystems, *Curr. Opin. Electrochem.*, 2019, **15**, 175–185.
11 D. G. Rackus, M. H. Shamsi and A. R. Wheeler, Electrochemistry, biosensors and microfluidics: a convergence of fields, *Chem. Soc. Rev.*, 2015, **44**, 5320–5340.
12 J. Hu, *et al.* Portable microfluidic and smartphone-based devices for monitoring of cardiovascular diseases at the point of care, *Biotechnol. Adv.*, 2016, **34**, 305–320.
13 K. Cheng, *et al.* Automated and rapid chemiluminescence immunoassay for cardiac troponin I based on digital microfluidics, *Microfluid. Nanofluid.*, 2023, **27**, 1–10.
14 A. H. C. Ng, *et al.* A digital microfluidic system for serological immunoassays in remote settings, *Sci. Transl. Med.*, 2018, **10**, 1–12.
15 R. P. S. De Campos, *et al.* 'plug-n-Play' Sensing with Digital Microfluidics, *Anal. Chem.*, 2019, **91**, 2506–2515.
16 G. W. H. Evans, *et al.* A portable droplet microfluidic device for cortisol measurements using a competitive heterogeneous assay, *Analyst*, 2021, **146**, 4535–4544.
17 M. Y. H. Tang and H. C. Shum, One-step immunoassay of C-reactive protein using droplet microfluidics, *Lab Chip*, 2016, **16**, 4359–4365.
18 C. A. Chen, *et al.* An electricity- And instrument-free infectious disease sensor based on a 3D origami paper-based analytical device, *Lab Chip*, 2021, **21**, 1908–1915.
19 F. Ozefe and A. Arslan Yildiz, Fabrication and development of a microfluidic paper-based immunosorbent assay platform (μPISA) for colorimetric detection of hepatitis C, *Analyst*, 2023, **148**, 898–905.
20 H. Fu, *et al.* Paper-Based All-in-One Origami Nanobiosensor for Point-of-Care Detection of Cardiac Protein Markers in Whole Blood, *ACS Sens.*, 2023, **8**, 3574–3584.
21 P. Kaewarsa, M. S. Schenkel, K. L. Rahn, W. Laiwattanapaisal and C. S. Henry, Improving design features and air bubble manipulation techniques for a single-step sandwich electrochemical ELISA incorporating commercial electrodes into capillary-flow driven immunoassay devices, *Analyst*, 2024, 2034–2044, DOI: 10.1039/d3an01704d.
22 A. Dobrea, N. Hall, S. Milne, D. K. Corrigan and M. Jimenez, A plug-and-play, easy-to-manufacture fluidic accessory to significantly enhance the sensitivity of electrochemical immunoassays, *Sci. Rep.*, 2024, **14**, 1–11.
23 K. Chandnani, *et al.* Technological advancement and current standing of microfluidic chip based devices for targeted analysis of biomarkers, *Microchem. J.*, 2023, **195**, 109532.
24 J. Horak, C. Dincer, E. Qelibari, H. Bakirci and G. Urban, Polymer-modified microfluidic immunochip for enhanced electrochemical detection of troponin i, *Sens. Actuators, B*, 2015, **209**, 478–485.
25 Y. Li, *et al.* Sensitive immunoassay of cardiac troponin I using an optimized microelectrode array in a novel integrated microfluidic electrochemical device, *Anal. Bioanal. Chem.*, 2020, **412**, 8325–8338.
26 H. J. Sheen, *et al.* Electrochemical biosensor with electrokinetics-assisted molecular trapping for enhancing C-reactive protein detection, *Biosens. Bioelectron.*, 2022, **210**, 114338.
27 N. H. Menon, Y. Beshai and S. Basuray, Fully Automated Microfluidic Electrochemical Platform as a Versatile Biosensor, *IEEE Sens. Lett.*, 2025, **9**(8), 1–4.
28 A. Sinha, *et al.* An integrated microfluidic system with field-effect-transistor sensor arrays for detecting multiple cardiovascular biomarkers from clinical samples, *Biosens. Bioelectron.*, 2019, **129**, 155–163.
29 A. Ecke, J. Bell and R. J. Schneider, *Sens. Diagn.*, 2023, **2**, 887–892.
30 J. Wu, F. Yan, J. Tang, C. Zhai and H. Ju, A disposable multianalyte electrochemical immunosensor array for automated simultaneous determination of tumor markers, *Clin. Chem.*, 2007, **53**, 1495–1502.
31 J. Wu, *et al.* A disposable electrochemical immunosensor for flow injection immunoassay of carcinoembryonic antigen, *Biosens. Bioelectron.*, 2006, **22**, 102–108.
32 H. Zhao, *et al.* Accessible detection of SARS-CoV-2 through molecular nanostructures and automated microfluidics, *Biosens. Bioelectron.*, 2021, **194**, 113629.
33 Z. Altintas, M. Akgun, G. Kokturk and Y. Uludag, A fully automated microfluidic-based electrochemical sensor for real-time bacteria detection, *Biosens. Bioelectron.*, 2018, **100**, 541–548.
34 Y. Uludag, *et al.*, An integrated lab-on-a-chip-based electrochemical biosensor for rapid and sensitive detection of cancer biomarkers, *Anal. Bioanal. Chem.*, 2016, **408**, 7775–7783.
35 S. B. Dulay, R. Gransee, S. Julich, H. Tomaso and C. K. O'Sullivan, Automated microfluidically controlled electrochemical biosensor for the rapid and highly sensitive detection of Francisella tularensis, *Biosens. Bioelectron.*, 2014, **59**, 342–349.
36 K. Kadimisetty, *et al.* Automated 3D-Printed Microfluidic Array for Rapid Nanomaterial-Enhanced Detection of Multiple Proteins, *Anal. Chem.*, 2018, **90**, 7569–7577.
37 K. A. Yang, *et al.* High-Affinity Nucleic-Acid-Based Receptors for Steroids, *ACS Chem. Biol.*, 2017, **12**, 3103–3112.
38 R. Sánchez-Salcedo, R. Miranda-Castro, N. De-los-Santos-Álvarez, M. J. Lobo-Castañón and D. K. Corrigan, Comparing nanobody and aptamer-based capacitive sensing for detection of interleukin-6 (IL-6) at physiologically relevant levels, *Anal. Bioanal. Chem.*, 2023, **415**, 7035–7045.
39 V. J. Vezza, *et al.* An electrochemical SARS-CoV-2 biosensor inspired by glucose test strip manufacturing processes, *Chem. Commun.*, 2021, **57**, 3704–3707.
40 P. Lasserre, *et al.* SARS-CoV-2 Aptasensors Based on Electrochemical Impedance Spectroscopy and Low-Cost Gold Electrode Substrates, *Anal. Chem.*, 2022, **94**, 2126–2133.
41 S. Hannah, *et al.* Rapid antibiotic susceptibility testing using low-cost, commercially available screen-printed electrodes, *Biosens. Bioelectron.*, 2019, **145**, 111696.
42 H. Ghorbanpoor, *et al.* A fully integrated rapid on-chip antibiotic susceptibility test – A case study for

Mycobacterium smegmatis, *Sens. Actuators, A*, 2022, **339**, 113515.

43 D. Wachholz Junior, R. G. Pontes, B. M. Hryniewicz and L. T. Kubota, Exploring a CRISPR/Cas12a-powered impedimetric biosensor for amplification-free detection of a pathogenic bacterial DNA, *Biosens. Bioelectron.*, 2025, **285**, 117607.

44 A. C. Lazanas and M. I. Prodromidis, Electrochemical Impedance Spectroscopy—A Tutorial, *ACS Meas. Sci. Au*, 2023, **3**, 162–193.